ANL/ED/CP-94693

CONF-9710102--

Selection and Microstructures of High Density Uranium Alloys*

by

M.K. Meyer, C.L. Trybus, G.L. Hofman, S.M. Frank and T.C. Wiencek

Engineering Division
Argonne National Laboratory
P. O. Box 2528
Idaho Falls, Idaho 83403-2528

Conference Paper to be submitted for presentation at the
International Meeting on Reduced Enrichment for Research and Test Reactors
Jackson Hole, WY.
October 5 - 10, 1997

*Work supported by the U.S. Department of Energy, RERTR, under Contract W-31-109-ENG-38.

DISCLAIMER

Selection and Microstructures of High Density Uranium Alloys

M.K. Meyer, C.L. Trybus, G.L. Hofman, S.M. Frank, and T.C. Wiencek

Argonne National Laboratory
Idaho Falls, ID
Argonne, IL

Work supported by the U.S. Department of Energy,
Office of Nonproliferation and National Security,
under Contract W-31-109-ENG-38

Twelve uranium alloys have been selected for incorporation into very high density aluminum dispersion fuel plates for irradiation testing. These alloys are (nominally) U-10Mo, U-8Mo, U-6Mo, U-4Mo, U-9Nb-3Zr, U-6Nb-4Zr, U-5Nb-3Zr, U-2Mo-1Nb-1Zr, U-6Mo-1Pt, U-6Mo-0.6Ru, U-6Mo-0.6Si, and U-10Mo-0.05Sn. The rationale for selection of these fuels based on gamma phase stability, reports of good irradiation performance, and high uranium density will be discussed. The microstructures of these fuels were examined by SEM/EDS and XRD at three stages during the powder fabrication process. Microstructures of selected alloys are discussed.

Presented at the 20th Annual Conference on
Reduced Enrichment for Research and Test Reactors
Jackson, WY (1997)

Introduction

Conversion of a number of research reactors to the use of LEU fuels (low-enriched uranium) requires that uranium densities of 8 to 9 g/cm^3 be incorporated into current dispersion fuel configurations.[1] It would be preferable to make this very high density fuel using commercial fuel fabrication technologies, which set a practical upper limit on fuel loading of approximately 55 volume percent. Given this practical constraint on fuel volume loading, fuel phases with uranium densities of at least 14.5 g/cm^3 must be used to fabricate this fuel. Two types of fuel are available that meet this density criterion. These are metallic uranium of low alloy content and the U_6Me class of high density intermetallics. In this class, U_6Fe and U_6Mn have been shown to have poor irradiation behavior[2], and it is likely that other U_6Me compounds will behave in a similar manner. The emphasis for US-RERTR advanced fuel development has therefore been placed on the development of metallic uranium alloy fuels.

Alloy Selection

Since little irradiation data exists on the performance of metallic fuels in the high burnup, low temperature range, it is advantageous to be able to screen many alloys in order to identify good performers. An irradiation test that has been designed to accomplish this task is currently underway in the Advanced Test Reactor (ATR).[3,4] Twelve fuel alloys and two intermetallic compounds were selected for irradiation to 40 and 80 atom percent burnup. The intermetallics are to be used as baseline reference materials and to investigate the behavior of alloy decomposition phases. Alloys were selected on the basis of γ phase stability, reports of good irradiation performance, and high uranium density. Other considerations were stability in contact with aluminum and the representation of a broad spectrum of alloy types. Molybdenum and niobium-zirconium are the most attractive alloying elements due to a large solubility range in the metastable γ phase and acceptable neutronic performance. The test matrix was built around these alloys and variants.

The fuel alloys selected for irradiation can be divided into four fuel types based on microstructure. These are given in Table I. The first type are alloys with fairly high alloying additions that are expected to remain in the metastable γ-phase (or a phase closely related to the γ-phase[5]) during fuel plate fabrication and prior to insertion in reactor. These alloys are listed in the left hand column of Table I.

Table I. Fuel alloys chosen for irradiation screening tests
(alloying element in wt%)

Most γ stable	Intermediate γ stability	Least γ stable ($\alpha + \gamma'$)	Precipitate Dispersion within Fuel Particles
U-10Mo	U-6Mo	U-5Nb-3Zr	U-10Mo-0.05Sn
U-8Mo	U-6Mo-1Pt	U-4Mo	U-6Mo-0.1Si
U-9Nb-3Zr	U-6Mo-0.6Ru	U-2Mo-1Nb-1Zr	
	U-6Nb-4Zr		

If the current hot rolling and extrusion processes are to be used to fabricate fuel plates, and a γ-phase alloy dispersion is to be the end product, then the γ-phase must remain stable for times on the order of hours at 400-500°C. There are several promising literature references to the γ-phase stability of U-Mo alloys. Repas, et al.[6] indicates that U-10Mo is stable for upwards of 8 hours at 490°C. The T-T-T (time-temperature-transformation) curve for U-10Mo is drawn for temperatures down to 300°C, and indicates γ phase stability for upwards of 800 hours at this temperature before start of formation of the γ' (U_2Mo) phase occurs. Other studies support the general conclusion of a very stable γ phase,[7,8,9] although there are differences in reported T-T-T curves. Of possible concern is the effect of the high surface area present in powders on transformation kinetics. Goldstein and Bar-Or[10] report very rapid transformation kinetics for U-10.8Mo powder at 500°C. U-8Mo begins to decompose from γ at times on the order of 10% of the time required for the start of U-10Mo decomposition.

The addition of zirconium to U-Nb alloys has a large effect on extending the metastability range. Thomas[11] indicates that a U-10Nb-4Zr alloy is γ-stable for 10 hours at 550°C, while a U-14Nb alloy transforms in less than 0.2 hours. Many studies have concentrated on the mechanical and corrosion resistance of U-7.5Nb-2.5Zr. Dean[12] studied the transformation behavior of U-7.5Nb-2.5Zr. The T-T-T diagram generated from this study consists of two overlapping C-curves. The upper curve has a nose at 525°C and 20 minutes, the lower curve at 350°C and three minutes. The upper C-curve approaches 650°C asymptotically, and there may be ample time for hot rolling somewhere in the ranges of $400°<T<500°C$ and $T>550°C$. T-T-T diagrams are also given by Karnowsky and Rohde,[13] Giraud-Heraud and Guillaumin,[14] and Vandermeer.[15] As in the case of U-Mo alloys, transformation times vary somewhat in these studies.

Despite a good deal of research on the properties and irradiation behavior of γ-phase alloys, there is little data that establishes the high-burnup, low-temperature swelling behavior. High temperature, low burnup data are common. It has been shown that γ-stable metallic fuels are more resistant to swelling than α-uranium based fuels under these irradiation conditions. Beghi[16] provides a summary of data for U-Mo alloys to ~1967. Data from Johnson and Holland[17] indicate that swelling decreases in direct proportion to molybdenum content for a variety of fission rates and temperatures from 480-700°C. Phillips[18] studied swelling as a function of burnup and peak fuel temperature for (initially γ-phase) U-9Mo. The fuel shows stable swelling behavior at $T<500°C$. At $T<425°C$ the fuel remained in the γ phase. It has also been shown that at irradiation temperatures less than 200°C, equilibrium α + γ' (U_2Mo) structures with sufficient alloy content to be quenchable to the metastable γ phase will revert to γ on irradiation to burnup on the order of 0.1%.[19,20] At temperatures above 370°C, ternary U-Nb-Zr alloys were shown to have much superior swelling resistance to binary U-Nb alloys.[21] Total burnup, however, was less than 1%. Less than 2% swelling of U-Nb alloys occurred at irradiation temperatures of 200°C.

The relatively high alloy content of the γ stable fuels leads to a decrease in neutronic efficiency due to lower specific fissile atom density and parasitic neutron absorption. In order to achieve a uranium density of 9 gU/cm^3, U-10Mo fuel plates would have to be loaded to 53 volume percent fuel. This loading is at the upper end of the practical limits for hot rolling, making hot rolling operations more prone to the production of defective plates. The second and third classes of alloys were thus selected to provide for higher fissile atom densities in the fuel particles by decreasing alloy content. Alloys in the second column of Table I are expected to partially transform from the γ-phase during fuel plate fabrication. It has been found that small ternary additions of Pt[22] and Ru[23] to U-Mo alloys act as powerful γ stabilizers, and these alloys have been included in the test matrix. A comparison of T-T-T curves for U-Mo-Pt, U-Mo-Ru, U-Mo and U-Nb alloys are shown in Figure 1. On an atom-per-atom basis, small additions have roughly twice the γ stabilizing effect of molybdenum when incorporated into ternary U-Mo-Ru alloys (Table II). Based on limited data, the effects due to platinum substitution for molybdenum may be even greater. The class of ternary alloys containing platinum and ruthenium seem to be the most promising in terms of the tradeoff between fissile atom density and gamma stability. Further investigation of the transformation behavior of an extended range of U-Mo-(Pt,Ru) alloy compositions is underway.

Table II. Gamma stabilizing effect of Ru and Pt in U-Mo-X Alloys[22,23]
(X equivalence to Mo atoms)

U-Mo-X alloys	X=Ruthenium		X=Platinum
	2 at%	4 at%	1 at%
Alloys with 14 at% Solute	2.4	1.7	
Alloys with 16 at% Solute	1.8	1.5	
Alloys with 18 at% Solute	1.7	1.3	≈4

Alloys in the third column of Table I represent materials with the highest density of uranium atoms. These alloys are expected to completely decompose to the equilibrium α + γ' (U_2Mo) during fuel plate fabrication, and then revert to the α + γ phases[24] at low burnup on irradiation. These alloys were included in the test matrix on the chance that irradiation behavior at a low temperature and in a dispersed configuration might be better than expected from bulk data.

The fourth class of alloys are U-Mo alloys with very small ternary additions of silicon and tin. These alloys are heat treated to produce a fine dispersion of intermetallic precipitates within individual fuel particles. The U-10Mo based alloy remains substantially γ phase on heat treating. Kramer and Johnston[25] reported swelling data from post irradiation annealing experiments of similar alloys after burnup on the order of 0.5 at%. Intermetallic precipitate density was on the order of 10^{18}-10^{19} m^{-3}. Figure 2 shows data for uranium, U-Mo, U-Mo-Sn, and U-Mo-Si alloys irradiated at 300° and 400°C.

Data at the lowest temperature point for each curve represents swelling observed in the as-irradiated condition. Data points at higher temperatures represent swelling after post-irradiation anneals for times of 5-72 hours. It can be seen that the ternary alloys were more resistant to swelling in reactor and during post irradiation anneals. This behavior may represent the effect of a stable fission gas bubble dispersion. All three U~10Mo alloys were more resistant to swelling in reactor and during post irradiation anneals than a U-4.4Mo alloy tested under the same conditions.

Microstructures of Selected Alloys

Fuel alloys were injection cast into rods form. After casting, alloys were wrapped in tantalum foil, encapsulated in evacuated stainless steel tubes and given a homogenization heat treatment at 900°C (in the γ-U phase field), followed by air cooling. Optical microscopy and SEM/EDS were used to examine the microstructures of the alloys in the as cast and homogenized states and the microstructures of the fabricated and blister annealed fuel plates. X-ray diffraction patterns were taken from polished and etched lateral cross sections of fuel pins and on the as-ground powder. The fuel pin samples proved to be less than ideal for this purpose. Excess grain growth during heat treatment resulted in some xrd patterns with distorted peak intensity ratios and 'missing peaks'. The terms γ and α are used to describe the nominal phases as fine structural detail could not be resolved. Powder diffraction patterns were diffuse, presumably due to extensive cold work during machining. It has often been noted that introducing cold work may cause reversion to the 'γ' phase. Attempts at quantifying lattice parameters and

Table III. Summary of Alloy Data

Alloy	Alloy phases[a]	Powder XRD	Reaction w/ Aluminum[b]
U-10 Mo	γ	γ + WC[c]	1
U-8Mo	γ	γ + WC	1
U-6Mo	γ	γ	3
U-4Mo	γ+d	γ (v. diffuse)	3
U-6Mo-0.6Ru	γ	γ	2
U-6Mo-1Pt	γ	γ + tr. WC	2
U-9Nb-3Zr	γ	γ + tr. WC	2
U-6Nb-4Zr	γ + d	γ	3
U-5Nb-3Zr	γ + α	γ (v. diffuse)	3
U-2Mo-1Nb-1Zr	α	α	4
U-10Mo-0.05Sn	γ	γ	1

a) Nominal phase by xrd and/or metallography in heat treated condition. d indicates decomposition products unidentified by xrd.

b) Numbers 1-4 indicate increasing severity of reaction with aluminum on microplate fabrication and blister anneal. 1=no reaction, 4= reaction with aluminum nearly complete.

c) Tungsten carbide was introduced on powder processing.[3]

calculating x-ray density gave values with large errors. Qualitatively, the phases present in the powder samples are as expected and listed in Table III, along with summary phase information. Descriptions of the microstructures of alloys prototypic of the first three columns of Table I are presented here.

U-2Mo-1Nb-1Zr: The as-cast alloy had a widely varying microstructure from top to bottom of the fuel pin. Shown in Figure 3(a) is an area near the bottom of the pin that exhibited acicular martensitic uranium.[26] The microstructure of other areas of the as cast fuel pin were similar in appearance to that of the sample after homogenization heat treatment. Micrographs in the homogenized condition (Figure 3(b)) show that decomposition has occurred on cooling from the γ phase field. The decomposition mechanism appears to be cellular. Prior γ grain boundaries are visible and act as cell nucleation sites. The xrd pattern (Figure 3(c)) shows a strong α-U (nominal phase) component in both the as-cast and homogenized states. The powder diffraction pattern shows that the powder is primarily α-U. A micrograph of the fuel zone of a fabricated and blister annealed U-2Mo-1Nb-1Zr microplate is shown in Figure 3(d). The fuel has almost completely reacted with the aluminum matrix to form a phase identified by EDS as $(U,Mo)Al_4$. Due to extensive reaction and plate swelling[27] on fabrication, this fuel was excluded from the irradiation test.

U-6Nb-4Zr: The as-cast sample shows signs of decomposition from γ-U (Figure 4(a)). X-ray diffraction (Figure 4(d)) indicates that the major phase is γ-U, with some minor reflections present that can be assigned to α-U. While, xrd patterns of the homogenized sample show that only γ-U is present, metallography indicates that the sample is in the early stages of decomposition from γ. In the homogenized sample, Figure 4(b), γ grain boundaries are visible. The unetched areas are likely γ-U; the etched areas are then a transformation product. There was no difference in composition by EDS between etched and unetched areas in the sample. This is not unexpected since decomposition from γ by either cellular or spinodal reactions involves formation of a lamellar substructure of the decomposition products. These lamella could not be resolved by SEM, and would likely appear as regions of average sample composition by EDS. On decomposition of γ phase U-Nb-Zr alloys it has been found[13] that the transformation path from the metastable phase to equilibrium involves different intermediates that depend on transformation conditions. The types of phases that form during air cooling of this composition are not well documented. It has been shown that quenched U-Nb-Zr alloys can form a structure with a slight tetragonal distortion and ordering, often referred to as γ_d°. The xrd pattern does not show the characteristic broad, low intensity reflections due to positional ordering[5,15] in the γ_d° intermediate, however, data quality may not be sufficient to detect these subtle changes. A micrograph of the fuel particles in a U-6Nb-4Zr microplate (Figure 4(c)) shows that considerable reaction with aluminum has occurred. EDS analysis of the reaction layer on the outside of the fuel particles gives a composition of $(U,Nb,Zr)Al_4$. There is a partially reacted zone between the particle surface and the unreacted core. As with all U-Nb-Zr alloys used in this experiment, some

particles appeared to have completely reacted with aluminum, while others were left unreacted. There is sufficient unreacted fuel present in the microplate to make a microstructural evaluation of the irradiation performance of the fuel alloy based on the behavior of fission gas bubbles.

U-9Nb-3Zr: An optical micrograph of the homogenized sample is compared with that of the as-cast pin in Figure 5. The as-cast pin shows a dendritic structure typical of alloys with a large liquidus gap that are cooled from the melt at intermediate quench rates. The homogenization heat treatment resulted in a microstructure that is much more uniform than seen in the as-cast sample. The homogenized sample resisted attempts at electrolytic etching. The microstructure appears to be largely homogeneous and single phase, with no evidence of banding (Figure 5(b)). Small precipitates on the order of 0.2-1 μm decorate the grain boundaries. Qualitative EDS analysis indicates that these particles are rich in niobium and zirconium and contain small amounts of silicon and aluminum, and are likely an oxide phase. XRD (Figure 5(c)) shows that this alloy is γ-U both as cast and in the homogenized and air quenched state. Considerable reaction also occurred between fuel and aluminum during the fabrication of U-9Nb-3Zr microplates, however, the volume of the reaction phase is qualitatively less than in the case of the lower U-Nb-Zr alloys.

Micrographs of the fuel zones of U-xMo series microplates are shown in Figure 6. Alloys containing 4 and 6 wt% molybdenum reacted extensively with the aluminum matrix. Alloys containing 8 and 10 wt% molybdenum showed only small, isolated areas of reaction on very small particles and thin areas on large particles. This implies that there is a critical molybdenum level between 6 and 8 wt% above which reaction of U-Mo alloys with aluminum is severely impeded. It is not as yet clear if this effect is due to the retention of γ-uranium during fabrication of the higher alloys.

Summary

Twelve candidate uranium alloys were selected for screening as dispersion fuels on the basis of literature reports of irradiation performance, density, and gamma phase stability. Alloys were injection cast into rod form and converted to powder by machining with a rotary file. X-ray diffraction patterns show that all alloy powders, with the exception of U-2Mo-1Nb-1Zr are nominally γ-uranium. Alloys were incorporated into miniature fuel plates, which were fabricated in a manner similar to commercial fuel. The molybdenum rich alloys U-8Mo and U-10Mo were the only alloys that did not react with aluminum during fabrication into fuel plates. Although substantial reaction did occur in other fuel plates, there is sufficient unreacted fuel phase to allow for microstructural evaluation of the irradiation performance of the allows.

Acknowledgements

The authors would like to acknowledge and thank C.R. Clark, J.D. Lawrence, P.A. Hansen, G. Knighton, R.W. Bratt, and M.D. Davis for contributions to alloy processing and fuel powder fabrication and E.L. Wood for metallography.

[1] J.L. Snelgrove, G.L. Hofman, M.K. Meyer, C.L. Trybus, T.C. Wiencek, "Development of Very-High-Density Low-Enriched-Uranium Fuels," submitted for publication in *Nuclear Engineering and Design*, March (1997).

[2] G.L. Hofman, R.F. Domagala, G.L. Copeland, "Irradiation Behavior of Low-Enriched U6Fe-Al Dispersion Fuel Elements,""*J. Nuc. Mat.,* 238-43 complete (1987)

[3] C.L. Trybus, T.C. Wiencek, M.K. Meyer, D.J. McGann, C.R. Clark, "Design and Fabrication of High Density Uranium Dispersion Fuels," this proceedings.

[4] S.L. Hayes, C.L. Trybus, M.K. Meyer, "Irradiation Testing of High Density Uranium Alloy Dispersion Fuels," this proceedings.

[5] H.L. Yakel, "Review of X-ray Diffraction Studies in Uranium Alloys," in Physical Metallurgy of Uranium Alloys (Proceedings of the Third Army Materials Technology Conference), eds. J.J. Burke, D.A. Colling, A.E. Gorum, and J. Greenspan, Brook Hill Publishing, Chestnut Hill, MA (1974).

[6] P.E. Repas, R.H. Goodenow, R.F. Hehemann, "Transformation Characteristics of U-Mo and U-Mo-Ti Alloys," Trans. Amer. Soc. Metals, **57** 150-63 (1964).

[7] R.F. Hills, D.R. Harries, D.J. Hodkin, M.B. Waldron, "Transformation of Metastable Phases in the Uranium-Molybdenum Alloy System," AERA M/R 2840, U.K.A.E.A. Harwell (1959).

[8] R.K. McGeary, "Development and Properties of Uranium-Base Alloys Resistant in High Temperature Water," USAEC Report WAPD-127, I. (1955).

[9] R.J. Van Thyne, D.J. McPherson, "Transformation Kinetics of Uranium-Molybdenum Alloys," *Trans. ASM* **49** 598-621 (1957).

[10] Y. Goldstein and A. Bar-Or, "Decomposition Kinetics of Gamma Phase Uranium Alloys Containing 8, 10.8, and 14.3 wt% Molybdenum," J. Inst. Metals **95** 17-21 (1967).

[11] D.E. Thomas, R.H. Fillnow, K.M. Goldman, J. Hino, R.J. Van Thyne, F.C. Holtz, D.J. McPherson, "Properties of Gamma-Phase Alloys of Uranium," Proceedings of the Second UN International Conference on the Peaceful Uses of Atomic Energy **5** P/1924 UN Geneva (1958).

[12] C.W. Dean, "A Study of the Time-Temperature-Transformation Behavior of a Uranium-7.5 Weight Percent Niobium-2.5 Weight Percent Zirconium Alloy," Oak Ridge Y-12 Plant Report Y-1694 (1969).

[13] M.M. Karnowsky, R.E. Rohde, "The Transformation Behavior of a U-16at%Nb-5.6at%Zr Alloy," *J. Nuc. Mat.* **49** 81-90 (1973/74).

[14] F. Giraud-Heaud, J. Guillaumin, "Formation de Phases de Transition Dans L'Alliage U-7.5Nb-2.5Zr," *Acta. Met.* **21** 1243-52 (1973).

[15] R.A. Vandermeer, "Recent Observations of Phase Transformations in a U-Nb-Zr Alloy," 219-57 in Physical Metallurgy of Uranium Alloys, Eds. J.J. Burke, D.A. Colling, A.E. Gorum, J. Greenspan, Brook Hill Publishing Co. (1976).

[16] G. Beghi, "Gamma Phase Uranium-Molybdenum Fuel Alloys," EUR 5053e Euratom (1968).

[17] M.P. Johnson and W.A. Holland, "Irradiation of U-Mo base Alloys," NAA-SR-6262 (1964).

[18] J.L. Phillips, "Full Power Operation of the Dounreay Fast Reactor," ANS-100 (1967).

[19] M.L. Bleiberg, L.J. Jones, B. Lustman, "Phase Changes in Pile Irradiated Uranium Alloys," *J. App. Phys.* **27** [11] 1270-83 (1956).
[20] M.L. Bleiberg, "Effect of Fission Rate and Lamella Spacing upon the Irradiation-Induced Phase Transformation of U-9 wt% Mo Alloy," *J. Nuc. Mat.* **2** 182-90 (1959).
[21] D.E. Thomas, R.H. Fillnow, K.M. Goldman, J. Hino, R.J. Van Thyne, F.C. Holtz, D.J. McPherson, "Properties of Gamma-Phase Alloys of Uranium," Proceedings of the Second UN International Conference on the Peaceful Uses of Atomic Energy **5** P/1924 UN Geneva (1958).
[22] R.J. Van Thyne, D.J. McPherson, "Transformation Kinetics of Uranium-Niobium and Ternary Uranium-Molybdenum -Base Alloys," *Trans. ASM* **49** 576-97 (1957).
[23] G. Cabane, G. Donzé, "Stabilisation de la Phase γ dans les Alliages Ternaires a Base D'Uranium-Molybdene," *J. Nuc. Mat.* **4** 364-73 (1959).
[24] V.D. Dmitriev, Sh. Ibragimov, A.G. Karmilov, "Effects of Neutron Irradiation on the Structure and Properties of Uranium Alloys Containing 0.6-9% by Weight Molybdenum," translated from *Atomnaya Energiya* **22** [6] 459-65 (1967).
[25] D. Kramer, W.V. Johnston, "Post Irradiation Annealing of Uranium-Molybdenum Ternary Alloys," J. Nuc. Mat. **9** [2] 213-215 (1963).
[26] R.F. Hills, B.R. Butcher, J.A. Heywood, "A Study of the Effect of Cooling Rate on the Decomposition of the γ-phase in Uranium Low Molybdenum Alloys," *J. Less Comm. Met.* **3** 155-69 (1961).
[27] T.C. Wiencek, M.K. Meyer, I. Prokofiev, and D.D. Keiser, "Reaction of Unirradiated High Density Fuels with Aluminum," this proceedings.

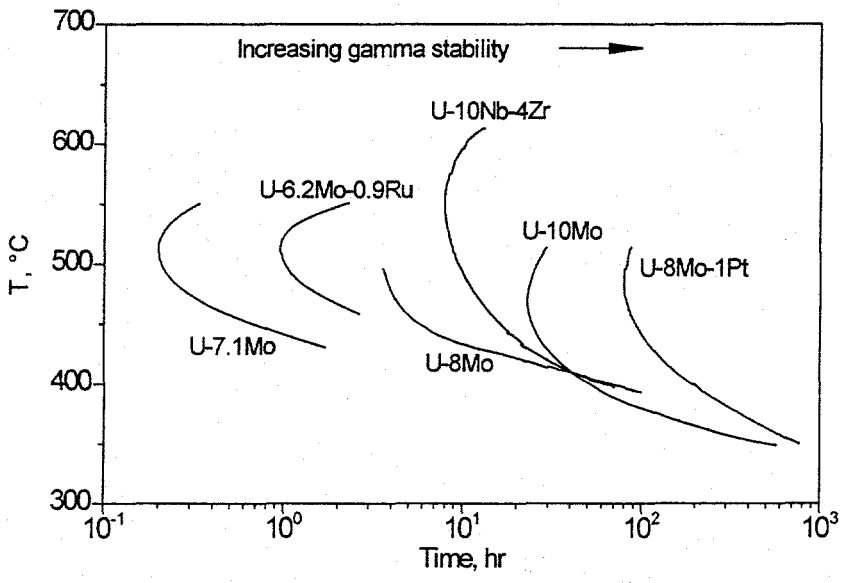

Figure 1. T-T-T curves for U-Mo, U-Mo-Pt, U-Mo-Ru, and U-Nb-Zr alloys.[9,21-23]

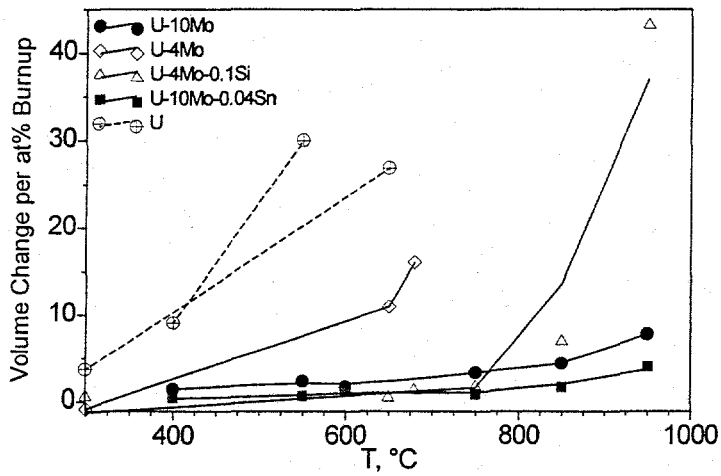

Figure 2. Swelling behavior of U-Mo alloys compared to U-Mo-Sn and U-Mo-Si alloys incorporating intermetallic dispersions.[25]

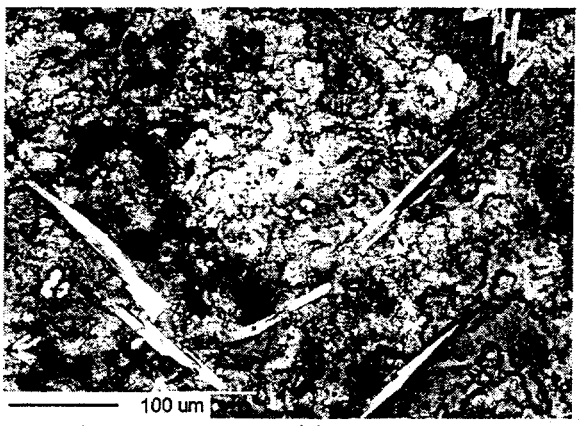

(a)

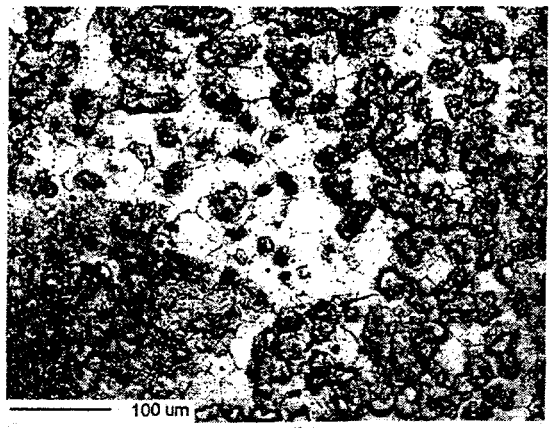

(b)

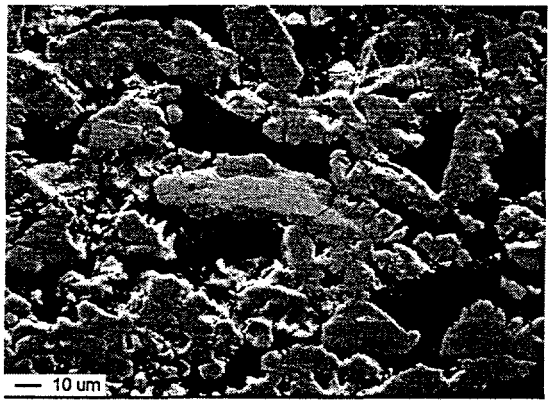

(c)

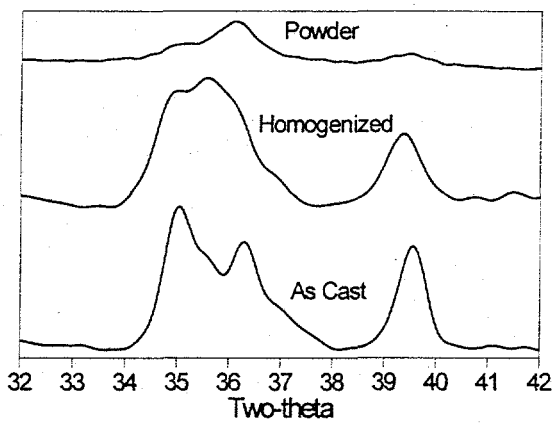

(d)

Figure 3. Microstructure of U-2Mo-1Nb-1Zr. (a) As cast. (b) After homogenization heat treatment at 900°C. (c) As fabricated microplate. (d) X-ray diffraction pattern showing strong reflections due to α-uranium.

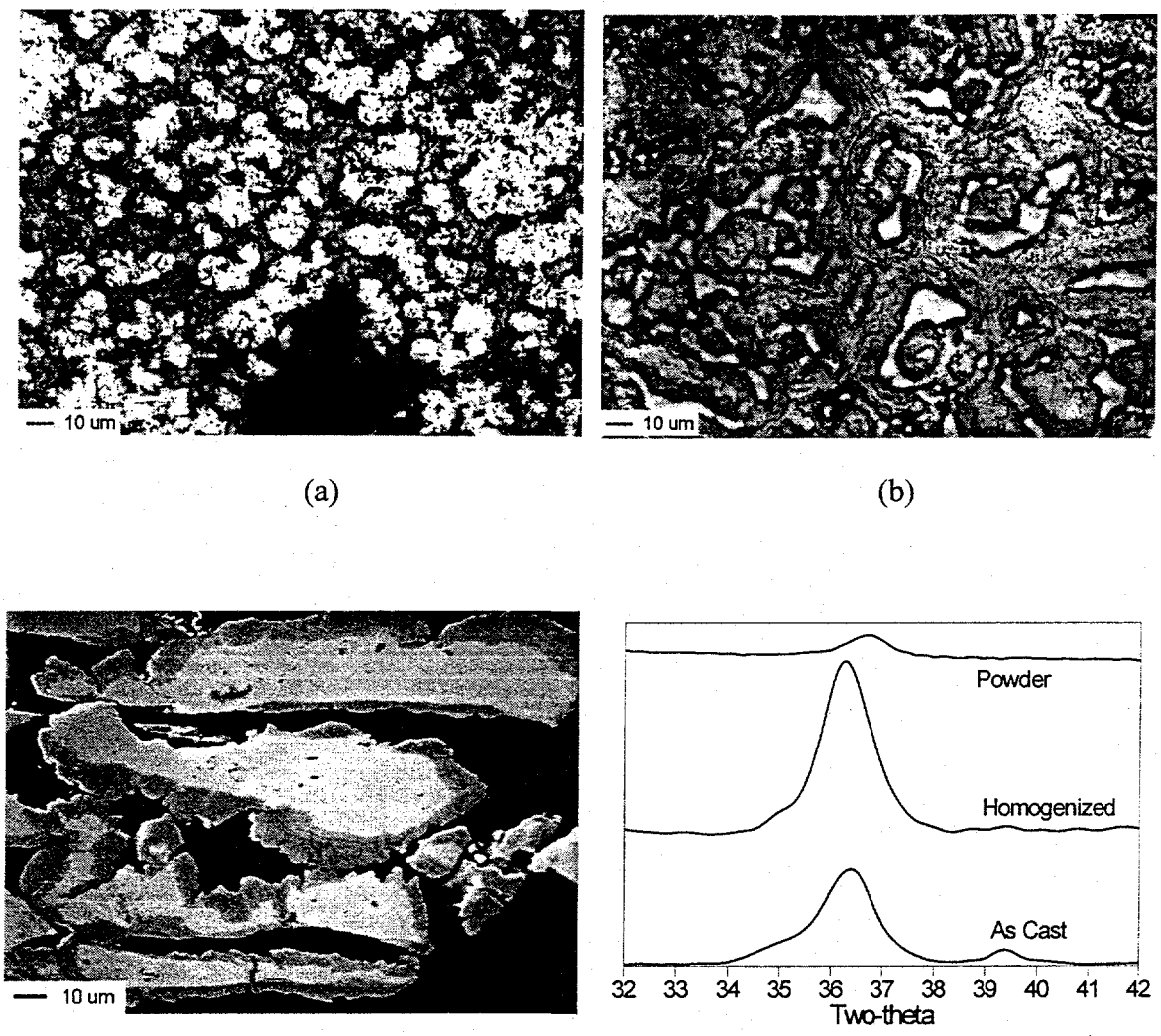

Figure 4. Microstructure of U-6Nb-4Zr. (a) As cast. (b) After homogenization heat treatment at 900°C. (c) As fabricated microplate. (d) X-ray diffraction pattern showing α-U + γ-U prior to heat treatment and γ-U after heat treatment.

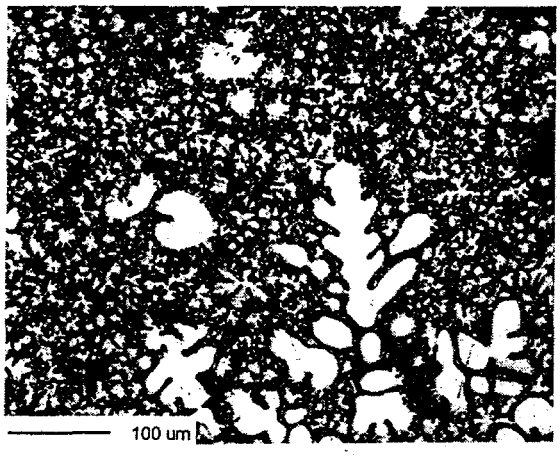

(a)

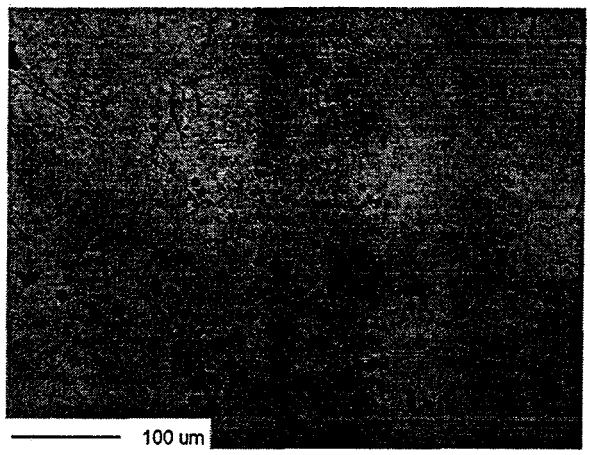

(b)

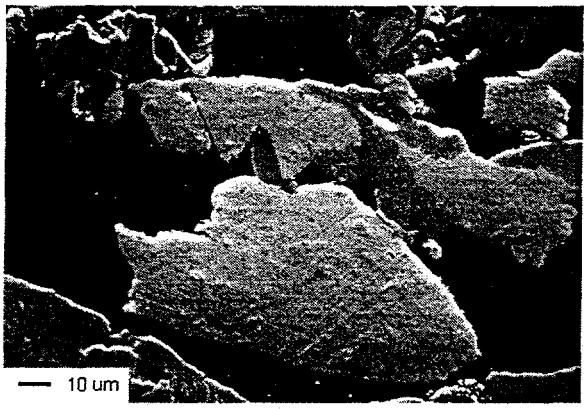

(c)

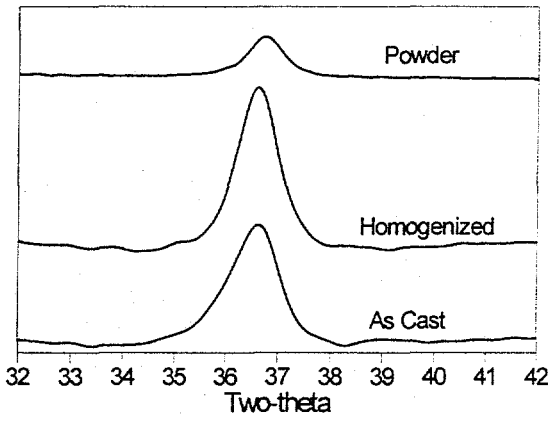

(d)

Figure 5. Microstructure of U-9Nb-3Zr. (a) As cast. (b) After homogenization heat treatment at 900°C. (c) As fabricated microplate. (d) X-ray diffraction pattern indicates γ-U in both as cast and homogenized conditions.

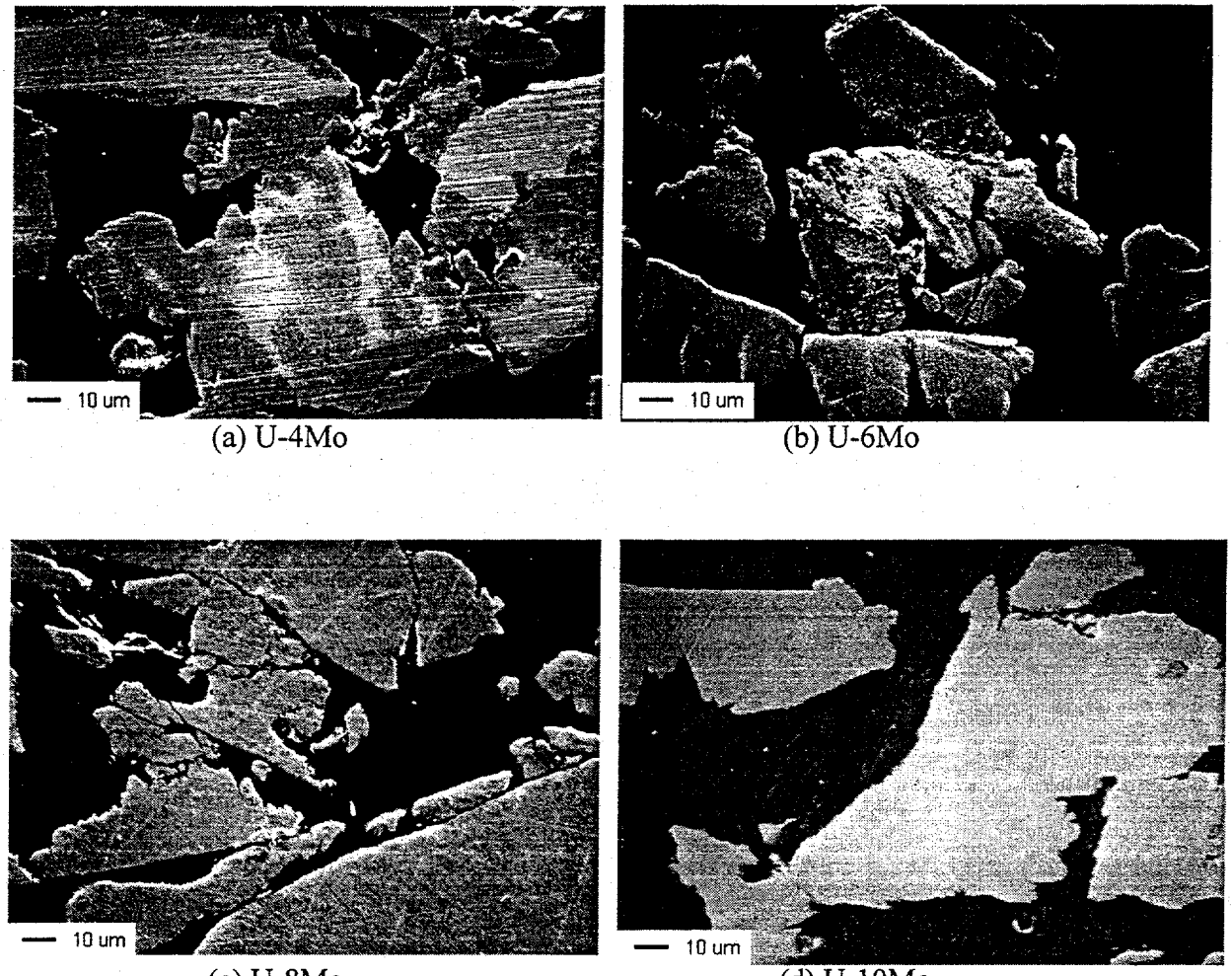

(a) U-4Mo (b) U-6Mo

(c) U-8Mo (d) U-10Mo

Figure 6. As fabricated U-xMo microplates. (a) U-4Mo and (b) U-6Mo have reacted with aluminum matrix. U-6Mo shows large tungsten carbide impurity top center. (c) U-8Mo and (d) U-10Mo show no reaction with aluminum.